

# Numerical simulation and hydrodynamic performance prediction for hydroplane longitudinal motion

Xiao Liang<sup>1\*</sup>, Wei Li<sup>2</sup>, Weitong Fan<sup>1</sup>, Guocheng Zhao<sup>1</sup>

<sup>1</sup> Transportation Equipments and Ocean Engineering College, Dalian Maritime University, China

<sup>2</sup> College of Environmental Science and Engineering, Dalian Maritime University, China

Received 1 February 2014, www.tsi.lv

---

## Abstract

Aiming at hydrodynamic performance prediction for hydroplane longitudinal motion, numerical simulation for a hydroplane motion was carried out by using VOF and RNG  $k-\epsilon$  model and solving Navier-Stokes equation under FLUENT software platform. Evolution of ship resistance was obtained as the velocity change, and flow field situation and dynamic pressure variation of hydroplane hull bottom were reflected intuitively. By comparing and analysing the results among numerical simulation calculation and ship model experiments and theoretical estimation, it was verified that hydrodynamic performance prediction for hydroplane longitudinal motion based on numerical simulation calculation under FLUENT is feasible and precise enough.

*Keywords:* numerical simulation; hydrodynamic performance prediction; hydroplane; FLUENT

---

## 1 Introduction

A hydroplane is a high-speed craft, which depends on fluid dynamic pressure generated on craft body during traveling to support most of the body weight. Hydroplane is widely used for such good hydrodynamic performances as speedability, maneuverability, etc. when traveling at a high speed. The research on this ship type has also become a key research field for international scholars [1, 2]. However, the research on hydrodynamic performance prediction for hydroplane motion is difficult, which is usually carried out through ship model tests and theoretical approximate formula estimations [3, 4].

In 2003, Davidson Laboratory obtained the influence law of various main elements on the motion in waves through a series of sea keeping tests to prismatic hydroplane model in regular head waves and irregular waves [5]. A. Rosen and K. Garne from Sweden Royal Institute of Technology made a research on the hydrodynamics and dynamic pressure of V-type ships during traveling at a high speed in still water through ship model tests [6]. The Ship and Ocean Engineering Dept. of UK University of Glasgow used CFD and ship model testing method to make a research comparison on forces on water surface speedboat in still water [7]. Dong Wencai, et. al. from China Naval Engineering University made a basic assumption for the longitudinal motion of speedboats in head waves, established a basic equation for longitudinal motion considering the influence of dynamic elevating force and proposed a new method of longitudinal motion forecasting—hydroplaning method. This method was verified to forecast the longitudinal

motions in head waves at medium and high navigational speeds [8]. In recent years, with the rapid development of computer technology, numerical simulation has also had a great development with various pieces of CFD software being more and more powerful in function and being increasingly higher in calculation accuracy. Using numerical simulation calculation method to simulate hydroplane motion condition and study hydrodynamic performance prediction has become a solution with a significant meaning.

In this paper, VOF method is used on FLUENT platform and RNG  $k-\epsilon$  model is combined to carry out numerical simulation calculation for hydroplane longitudinal motion by solving Navier-Stokes equation. Thereby the law of navigational resistance of hydroplane varying with the navigational speed is obtained and a comparison is made between the calculation results with FLUENT and the values of ship model test and theoretical estimation. The pressure variations on hydroplane hull bottom and the variations of flow field around hydroplane are investigated.

## 2 Control Equation and Numerical Calculation Method

For incompressible viscous flow under a typical Cartesian coordinate system, the influence of density impulsion is neglected and the time mean continuity equation, Reynolds equation in the form of tensor can be written as:

---

\* Corresponding author - Tel: +86-0411-84727985; fax: +86-0411-84725960; E-mail: liangxiao19801012@126.com

$$\frac{\partial \rho}{\partial t} + \frac{\partial}{\partial x_i}(\rho u_i) = 0, \quad (1)$$

$$\frac{\partial(\rho u_i)}{\partial t} + \frac{\partial}{\partial x_j}(\rho u_i u_j) = -\frac{\partial p}{\partial x_i} + \frac{\partial}{\partial x_j} \left( \mu \frac{\partial u_i}{\partial x_j} - \overline{\rho u_i u_j} \right) + S_i, \quad (2)$$

where  $i, j = 1, 2, 3$ ;  $\rho$  is the fluid density;  $\mu$  is the dynamic viscosity coefficient;  $u_i, u_j$  are the time mean values of speed components;  $u'_i, u'_j$  are the impulse values of speed components;  $p$  is the time mean value of pressure;  $S_i$  is general source item of momentum equation. The overline “—” means the time mean of physical quantities.

In RNG  $k-\varepsilon$  model, the influence of small dimension is embodied in large dimension motion and corrected viscosity item to remove small dimension motion from the control equation systematically. The  $k$  equation and  $\varepsilon$  equation are obtained:

$$\frac{\partial(\rho k)}{\partial t} + \frac{\partial(\rho k u_i)}{\partial x_i} = \frac{\partial}{\partial x_j} \left( \alpha_k \mu_{eff} \frac{\partial k}{\partial x_j} \right) + G_k + \rho \varepsilon, \quad (3)$$

$$\frac{\partial(\rho \varepsilon)}{\partial t} + \frac{\partial(\rho \varepsilon u_i)}{\partial x_i} = \frac{\partial}{\partial x_j} \left( \alpha_\varepsilon \mu_{eff} \frac{\partial \varepsilon}{\partial x_j} \right) + C_{1\varepsilon}^* \frac{\varepsilon}{k} G_k - C_{2\varepsilon} \rho \frac{\varepsilon^2}{k}, \quad (4)$$

where  $k$  is the turbulence kinetic energy;  $\varepsilon$  is the turbulence kinetic energy loss rate.

$$\mu_{eff} = \mu + \mu_t, \quad \mu_t = \rho C_\mu \frac{k^2}{\varepsilon}, \quad C_\mu = 0.0845,$$

$$\alpha_k = \alpha_\varepsilon = 1.39, \quad C_{1\varepsilon}^* = C_{1\varepsilon} - \frac{\eta(1 - \eta/\eta_0)}{1 + \beta\eta^3}, \quad C_{1\varepsilon} = 1.42,$$

$$C_{2\varepsilon} = 1.68, \quad \eta = (2E_{ij} \cdot E_{ij})^{1/2} \frac{k}{\varepsilon}, \quad E_{ij} = \frac{1}{2} \left( \frac{\partial u_i}{\partial x_j} + \frac{\partial u_j}{\partial x_i} \right),$$

$$\eta_0 = 4.377, \quad \beta = 0.012$$

In comparison with standard  $k-\varepsilon$  model, RNG  $k-\varepsilon$  model consider the rotation in average flow and swirling flow by correcting the turbulence kinetic energy viscosity. An item was added in  $\varepsilon$  equation to reflect the time mean strain of main flow  $E_{ij}$ . The item generated in RNG  $k-\varepsilon$  model is not only related to the flow condition, but also the function of space coordinates in the same question. As a result, flows with a high strain and highly bent flow lines can be treated better. As RNG  $k-\varepsilon$  model is effective for sufficiently developed turbulence, and flows near walls has a low Re number where the turbulence is not sufficiently developed, with the influence of turbulence impulsion being not so high as that of molecular viscosity, no calculation can be made with that model in this area and a special means of

treatment must be used. Here the wall function method is used to treat the flows near walls.

For free surface treatment questions, VOF method is selected in this paper [9]. VOF constructs and tracks a free surface according to the function  $F$  of volume taken by a fluid in grid cells at different times. For a space area containing a fluid of both gaseous and liquid phases, scalar function  $f$  is defined, with  $f$  value being 1 in case of liquid space points existing and being 0 for other points not occupied by liquid. Integrate  $f$  value on grid cells and divide this integration value by cell volume to obtain the average value of  $f$  for cells, that is, cell volume taken by liquid in grid cells, which is defined as  $F$ . If  $F = 1$  in a grid cell at some moment, it means that the grid cell is totally occupied by the fluid of a designated phase, being a fluid cell. If  $F = 0$ , that cell is totally occupied by the fluid of another phase. When  $0 < F < 1$ , the cell is a boundary cell containing materials of both phases. The equation that function  $F$  satisfies:

$$\frac{\partial F}{\partial t} + u \frac{\partial F}{\partial x} + v \frac{\partial F}{\partial y} + w \frac{\partial F}{\partial z} = 0. \quad (5)$$

### 3 Establishment and Setup of Calculation Model

The study object is a model “USV-3” used in hydroplane towing test. The ship model is a wooden model with a ground smooth surface sprayed with paint and the hull is naked. Through inspection, it is found to meet the tolerance standard in “Hydroplane Model Resistance Testing Method”. The model displacement  $\Delta = 66\text{kg}$ , the scale ratio  $\lambda = 1:4.58$ , the model length  $L_{OA} = 2.4\text{ m}$  and the molded breadth  $B = 0.735\text{ m}$ .



FIGURE 1 Hydroplane model in towing test

As the hydroplane molded lines are complicated and mostly three-dimensional curves, it is difficult to generate a curved surface directly in the pre-treatment software GAMBIT, Maxsurf software is used first to generate three-dimensional curves with surfaces and bodies being generated in GAMBIT and a calculation model for hydroplane is eventually obtained (as shown in figure 2).

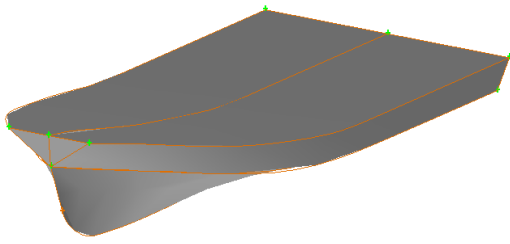


FIGURE 2 Calculation model of hydroplane

After a solid model is established in GAMBIT, adequate control field is selected according to the dimensions. According to the needs of flow field simulation calculation and by making reference to related literatures and experience from it, the control field is a rectangular body. The following scheme is used to set up the scope of calculation control field and the position of the ship model in the control field: the front end of the control field is at a location of  $2 L_{OA}$  from the bow, and the back end is at a location of  $3.75 L_{OA}$  from the stern, the uppermost boundary is at a location of  $0.75 L_{OA}$  above the keel and the lowermost boundary is at a location of  $2 L_{OA}$  below the keel and both sides are at the locations of  $2 L_{OA}$  from the mid-section on the right and left. As the navigational speed of the hydroplane is high, there will be a long wake. Therefore, in order to capture the wake well, the control body is extended to make the back end locate at  $5 L_{OA}$  from the stern. The solid ship model is 2.4m long, from which the length, width and height of the calculation control field obtained are 19.2 m, 9.6 m and 6.6 m respectively. As the model is symmetrical in relation to the longitudinal mid-section, half can be taken for the purpose of calculation. To simplify the model establishment process, the coordinate origin is set up at the lowest point of the stern, the direction of axis x pointing at the bow is positive, the direction of axis y pointing at the starboard is positive and the up direction of axis z is positive. The ship model position in the control field and the condition of control body is shown in figure 3.

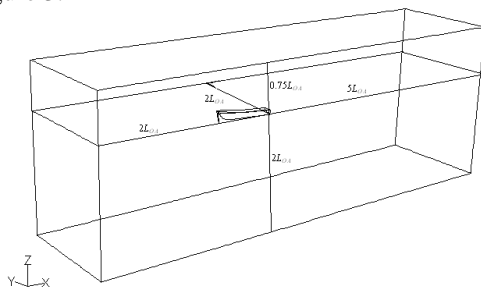


FIGURE 3 Ship model position of in the control field

Grid division is the most difficult part in establishing the mathematical model. How well the grid cells are divided not only determines if a correct solution can be obtained, but also determines the length of time to get the solution. As the grids divided in calculation vary greatly in volume from the location near the craft to the location far away from the craft, both non-structured and

structured grids are used in this paper. In consideration of computer calculation performance limitations and that the grids divided must change continuously in volume and there should not be too many grids and basic and key information on the flow field must be reflected, the control field is divided into several sub-fields in this paper, with non-structured grids being used near the craft and structured grids being used in a far location; the continuity of the grids between the sub-fields are controlled through the surface grids on the intersecting surfaces. Thus not only the need for calculation accuracy is ensured, but also the number of grids is reduced substantially and the calculation time is saved.

With regard to the locations containing a lot of small surfaces on the surface of craft body, those parts on the surface of the craft body with a small curvature variation are synthesized into larger surfaces first to reduce the difficulty in grid division. As the surface of the craft body is mostly composed of three-dimensional curved surfaces, it is difficult to generate structured grids near it and therefore surface grids are divided first on the surface of the craft body in which multiple verifications are necessary to find a suitable grid dimension. To facilitate body grid division near the craft body, we choose to use triangular surface grids on the surface of the craft body, and use tetrahedron non-structured grids near the craft body. To use quadrilateral grids on the surfaces of the calculation field can generate hexahedron structured grids in most areas in the control field except the locations near the craft body. The ratio between structured and non-structured grids will have a great influence on the calculation speed and quality. Generally, the use of non-structured grids should be reduced as possible as reasonably practical.

The areas near the craft body are important areas for the calculation study, where the density and quality of grids have a direct influence on the calculation results. In this paper, the method of increasing local grid density is used to refine grids and heighten the calculation accuracy. Grids of less density are used in areas farther away from the craft body and attention is paid to maintaining the grid density transition continuity. In dividing grids, the hexahedron structured grids in the far craft fields around are divided first and the tetrahedron non-structured grids near the craft are divided at last. This is favourable to grid transition between the sub-fields in the calculation field. The grid division in the control field is shown in figure 4.

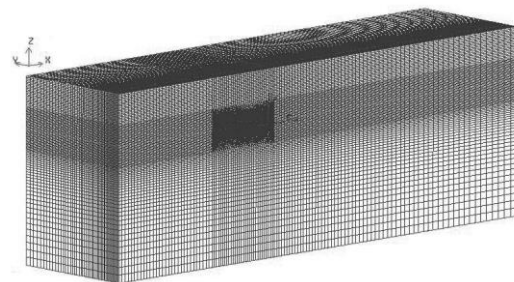


FIGURE 4 Grid division in calculation control field

**4 Control Equation and Numerical Calculation Method**

Numerical simulation calculation of hydroplane longitudinal motion is done on the FLUENT platform. Numerical simulations are made to the flow fields when a hydroplane makes even-speed longitudinal motion at five different navigational speeds, and a calculation study is made on the resistance. It is necessary to note that the corresponding trim angles and drafts of hydroplane at different navigational speeds can be obtained through ship model testing and theoretical analysis and are embodied in both GAMBIT modelling and FLUENT numerical calculation, which are not described in detail herein.

As shown in table 1 are the resistance value  $R_d$  and resistance coefficient  $C_d$  calculated by FLUENT and the comparison with ship model test values and the values estimated by applying empirical formulas. We can see that the resistance value  $R_d$  increases with navigational speed  $V$  or Froude number  $Fr_v$ , corresponding with the actual situation. The corresponding resistances calculated by FLUENT and the estimated resistance values at different speeds have no much difference, with the error between the corresponding calculated value and estimated value at 5 m/s being the largest as 3.56%.

TABLE 1 Resistance calculation comparison

Speed $v$ [m/s]	5	6	7	8	9
$Fr$	2.51	3.01	3.52	4.02	4.52
FLUENT value $F_R$ (N)	91.44	101.66	113.57	124.45	149.39
Resistance coefficient $C_d$	0.0084	0.0079	0.0053	0.0048	0.0046
Empirical estimation value (N)	102.31	104.06	111.28	123.96	141.25
Ship model test value (N)	94.82	100.40	111.32	126.86	147.06
Error in relation to test values %	-3.56	1.25	2.02	-1.9	1.59

Figure is the curve for FLUENT calculated values, test values, empirically estimated value varying with speeds. From the changing trends of the curves, they meet basically the law of resistances varying with speeds for hydroplane in a hydroplaning condition. Therefore, it is practical to apply FLUENT software to predict the resistance performances of a hydroplane in longitudinal motion and the accuracy is very high.

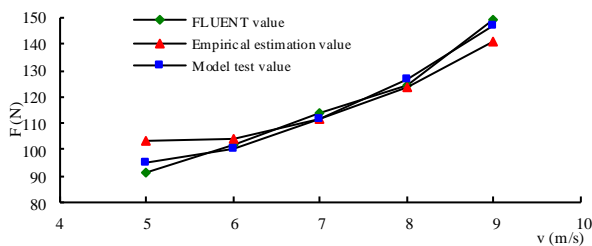


FIGURE 5 Curves for resistance varying with speed

The following is an investigation of the flow field change in numerical simulation process for hydroplane longitudinal motion. Figure 6(a)~(d) are cloud charts of volume fraction for the two phases of air and water on water surface varying with speeds, from which we can see intuitively the wake field varies with speed.

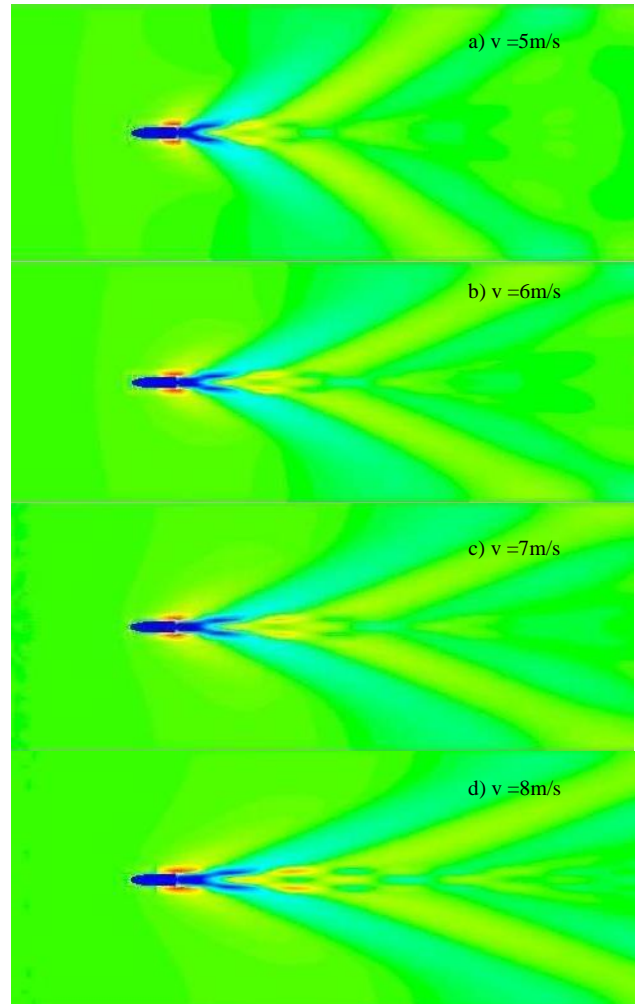


FIGURE 6 Cloud charts of volume fraction for the two phases of air and water on water surface varying with speed

Figure 7(a) ~ (d) are cloud charts of dynamic pressure on the hull bottom of hydroplane. As the navigational speed increases, the dynamic pressure on the hydroplane hull bottom increases. The dynamic pressure is a main reason for hydroplane to generate elevating force. Therefore, it indicates that the elevating force of the hydroplane increases with the navigational speed and this corresponds with the actual situation.

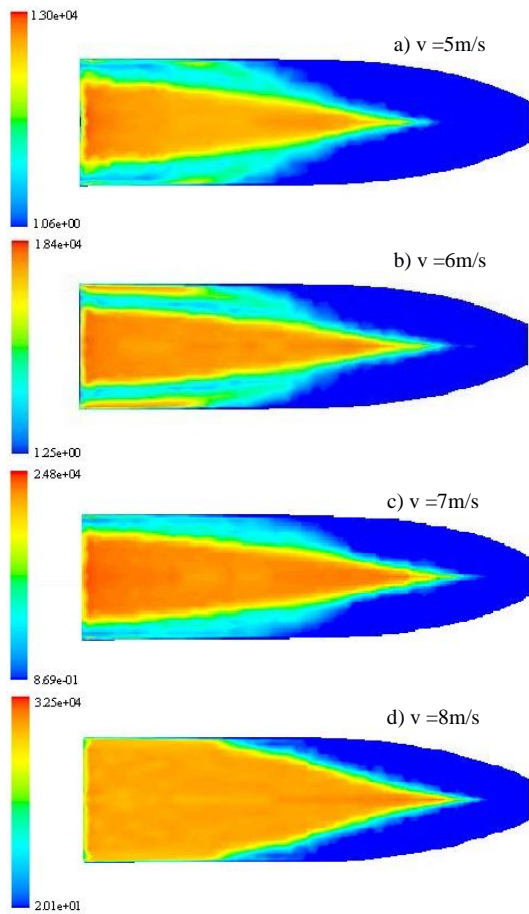


FIGURE 7 Cloud charts of dynamic pressure on hydroplane hull bottom varying with speed

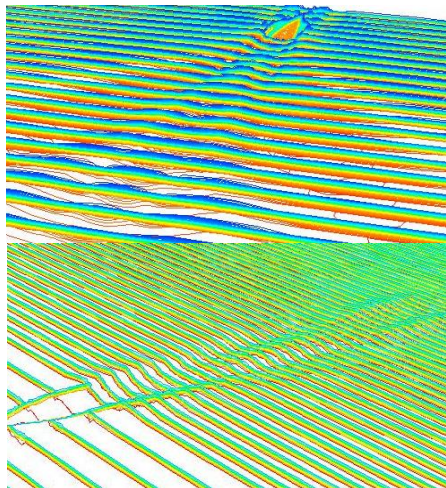


FIGURE 8 Wake flow of hydroplane motion

Figure 8 shows the change of wake flow during hydroplane longitudinal motion. From the simulation of flow field, the method can simulate wake flow of hydroplane motion well.

**4 Conclusions**

Aiming at hydrodynamic performance prediction for hydroplane longitudinal motion, numerical simulation for a hydroplane motion was carried out on FLUENT software platform. The law that the navigational resistance of hydroplane varies with the navigational speed is obtained. The variation of the flow field around hydroplane and the variation of the pressure on the hydroplane hull bottom are truly reflected. By comparing FLUENT calculated results and ship model test values and theoretically estimated values, it is proved that it is feasible and highly accurate to simulate water surface hydroplane motion and study the hydrodynamic performances on FLUENT platform.

**Acknowledgments**

This work is supported by the National Natural Science Foundation of China (Grant No. 51209025, 51379026) and Fundamental Research Funds for the Central Universities of China (Grant No. 3132014067, 3132013328).

**References**

- [1] Wang B. 2008 *Marine Equipment/Materials & Marketing* 2 4-17
- [2] Wu Y S, Ni Q J, Ge W Z. 2008 *Journal of Ship Mechanics* 12(6) 1014-31
- [3] Peng G W 2003 *Journal of Wuhan Institute of Shipbuilding Technology* 3 32-35
- [4] Xu Y L, You D D. 2009 *Ship & Boat* 20(4) 4-7
- [5] Y.Ikeyda, T.Katayama 2000 *Physical & Engineering Sciences, Philosophical Transactions of The Royal Society (A)* 358(1771) 1905-15
- [6] A Rosen, K Garne 2004 *Transaction of the Royal Institute of Naval Architects* 299-308
- [7] Tveitnes T, Fairlie-Clarke A C, Varyani K S 2008 *Ocean Engineering* 35(14) 1463-78
- [8] Dong W C, Liu Z H, Wu X G, Yue G Q 2007 *Journal of Ship Mechanics* 11(1) 55-61
- [9] Wang F J 2004 *The Analysis of Computational Fluid Dynamics-Principles and Applications of CFD Software* Tsinghua University Press: Beijing (in Chinese)

Authors	
	<p><b>Xiao Liang, born in 1980, China</b></p> <p><b>Current position, grades:</b> Dr. Liang is the senior member of International Association of Computer Science and Information Technology, and the member of Royal Institute of Naval Architect</p> <p><b>University studies:</b> doctor degree in Design and Construction of Naval Architecture and Ocean Structure, Harbin Engineering University, Harbin, China, 2009</p> <p><b>Scientific interest:</b> major field of study is hydrodynamics and underwater vehicles. One of his current jobs is Reliability Analysis of AUV Control System cooperating with State Key Laboratory of AUV, China. His current research interests include modelling, simulation and intelligent control of the AUV with fins</p> <p><b>Publications:</b> more than 20 papers in journals and conferences</p>
	<p><b>Wei Li, born in 1980, China</b></p> <p><b>Current position, grades:</b> One of her current jobs is Forecast and Emergency Response of Ship Oil Spill.</p> <p><b>University studies:</b> received doctor degree in Environment Science and Technology, Harbin Institute of Technology, Harbin, China, 2008.</p> <p><b>Scientific interest:</b> major field of study is hydrodynamics and numerical analysis. Her current research interests include modelling and simulation.</p> <p><b>Publications:</b> more than 20 papers in journals and conferences.</p>
	<p><b>Weitong Fan, born in 1989, China</b></p> <p><b>Current position, grades:</b> Now he is the postgraduate of Dalian Maritime University</p> <p><b>University studies:</b> received bachelor degree in Naval Architecture and Ocean Engineering, Dalian Maritime University, Dalian, China, 2009.</p> <p><b>Scientific interest:</b> major field of study is hydrodynamic performance of the ship.</p>
	<p><b>Guocheng Zhao, born in 1992, China</b></p> <p><b>Current position, grades:</b> He majors in Naval Architecture and Ocean Engineering in Dalian Maritime University as a junior student. He is the squadron commissary in charge of studies. He has finished two national innovation projects, two provincial innovation projects during the undergraduate and he is elected as Dalian Merit Student and Excellent Student Cadre for his active performance in study and work.</p>